DFT stimulation and experimental insights of chiral Cu(II)-salen scaffold within the pocket of MWW-zeolite and its catalytic study

Pratikkumar Lakhani[a], Darshil Chodvadiya[b], Prafulla K. Jha[b], Vivek Kumar Gupta[c], Damian Trzybiński[d], Krzysztof Wozniak[d], Krzysztof Kurzydłowski[e], U. K. Goutam[f], Himanshu Srivastava[g], Chetan K. Modi[a,*]

[a]*Applied Chemistry Department, Faculty of Technology & Engineering, The Maharaja Sayajirao University of Baroda, Vadodara, Gujarat-390001, India*
[b]*Department of Physics, Faculty of Science, The Maharaja Sayajirao University of Baroda, Vadodara, Gujarat-390002, India*
[c]*Department of Physics, University of Jammu, Jammu, Jammu and Kashmir-18006, India*
[d]*Biological and Chemical Research Centre, Faculty of Chemistry, University of Warsaw, Żwirki i Wigury 101, 02-089 Warszawa, Poland*
[e]*Materials Design Division, Faculty of Materials Science and Engineering, Warsaw University of Technology, 141 Wołoska Str., 02-507, Warsaw, Poland*
[f]*Technical Physics Division, Bhabha Atomic Research Centre, Mumbai-400085, India*
[g]*Synchrotrons Utilisation Section, Raja Ramanna Centre for Advanced Technology, Indore 452013, India*

Supporting Information

Table of Contents

1. General Information:

SiO2, HMI, Copper(II) acetate, (-)-trans-1,2-diaminocyclohexane, salicylaldehyde and MeOH was procured from Merck. While, some other chemicals such as aldehydes, ethyl acetoacetate and urea were procured from Loba Chemie, India. all of these reagents are of analytical grade and used as received without further purification.

2. Characterization's Techniques Information

For the characterization of as-prepared materials such as MWW zeolite, Cu(II) MWW zeolite and encapsulated chiral Cu(II) salen different physicochemical techniques have been employed. XPS spectra were performed on Specs, Phoibios 225 spectrometer with Al Kα radiation (1486.6 eV), Synchrotrons Utilisation Section, Raja Ramanna Centre for Advanced Technology, Indore, India. The structure determinations of as-prepared materials were performed on Bruker AXS D8 Advance X-ray powder diffractometer with a CuKα (λ=1.54058) target and movable detector, which scans the intensity of diffracted radiation within the range of 5°–80° as a function of the angle 2θ between the incident and diffracted beams. Field Emission Scanning Electron Microscopes (FE-SEM), the images were taken at 5 keV and as-prepared materials was performed on Model FE-SEM: Auriga HT Make: Carl Zeiss Model at Synchrotrons Utilisation Section, Raja Ramanna Centre for Advanced Technology, Indore, India. The images were taken at 5 keV. BET surface area and pore size distribution measure on micromeritics. FTIR spectra of as prepared materials were performed in the range: 4000-400 cm^{-1} on a model: FTIR - 8400S Shimadzu using KBr pellets. EDX analysis on JSM-IT800 Schottky Field Emission Scanning Electron Microscope, JEOL at The department of Metallurgical engineering, Faculty of Technology & Engineering, The Maharaja Sayajirao University of Baroda, Vadodara, India.

3. Spectral Data for chiral salen ligand

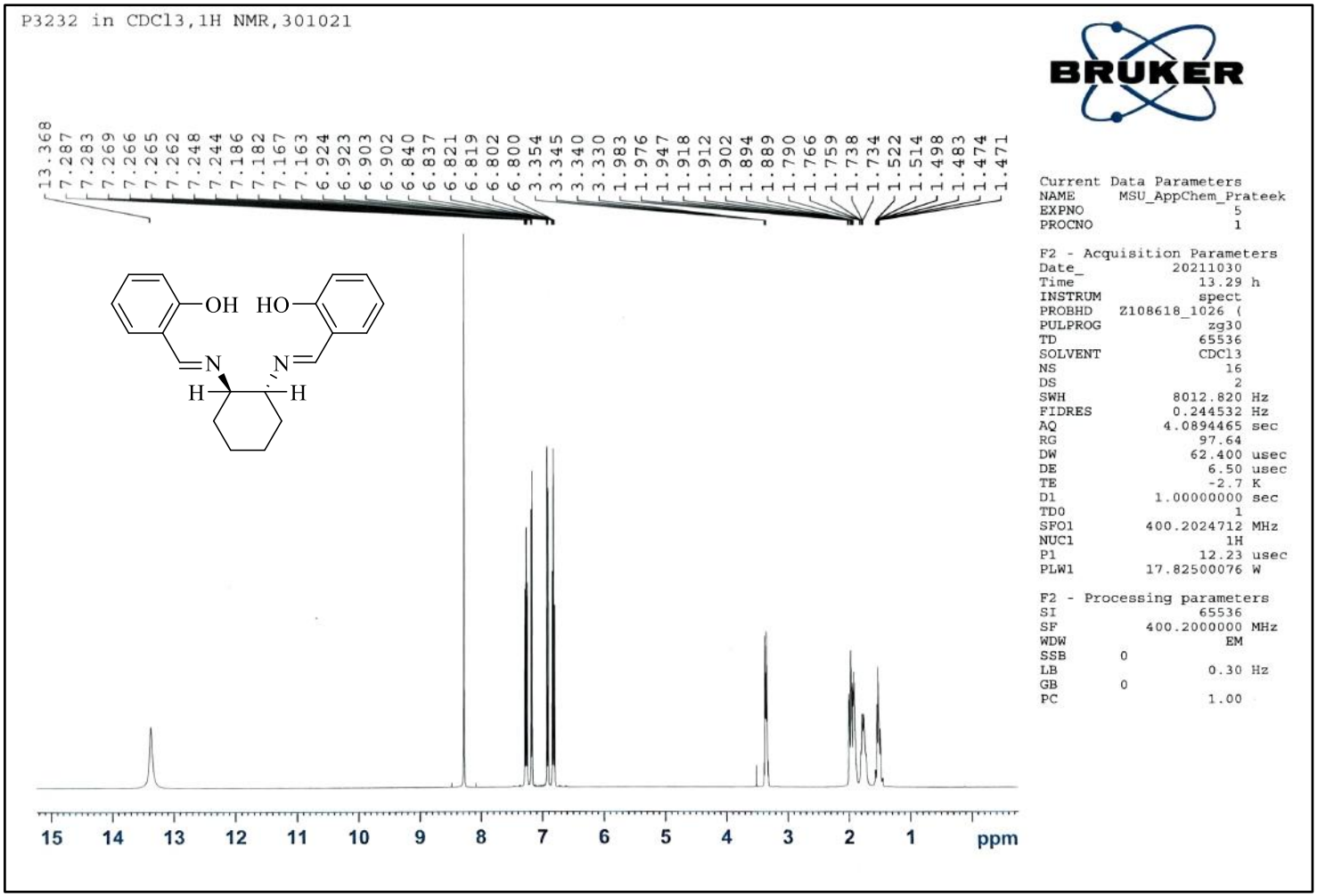

Fig. S1. ^{1}H NMR spectra of the chiral salen ligand.

^{1}H NMR spectra of the salen complex. ^{1}H NMR (400 MHz, $CDCl_3$): δ (ppm) = 13.36 (s, 1H), 8.31 (s, 1H), 7.28 (t, 1H), 7.18 (d, 1H), 6.92 (d, 1H), 6.83 (t, 1H), 3.35 (dd, 1H), 1.4-1.98 (m, 4H).

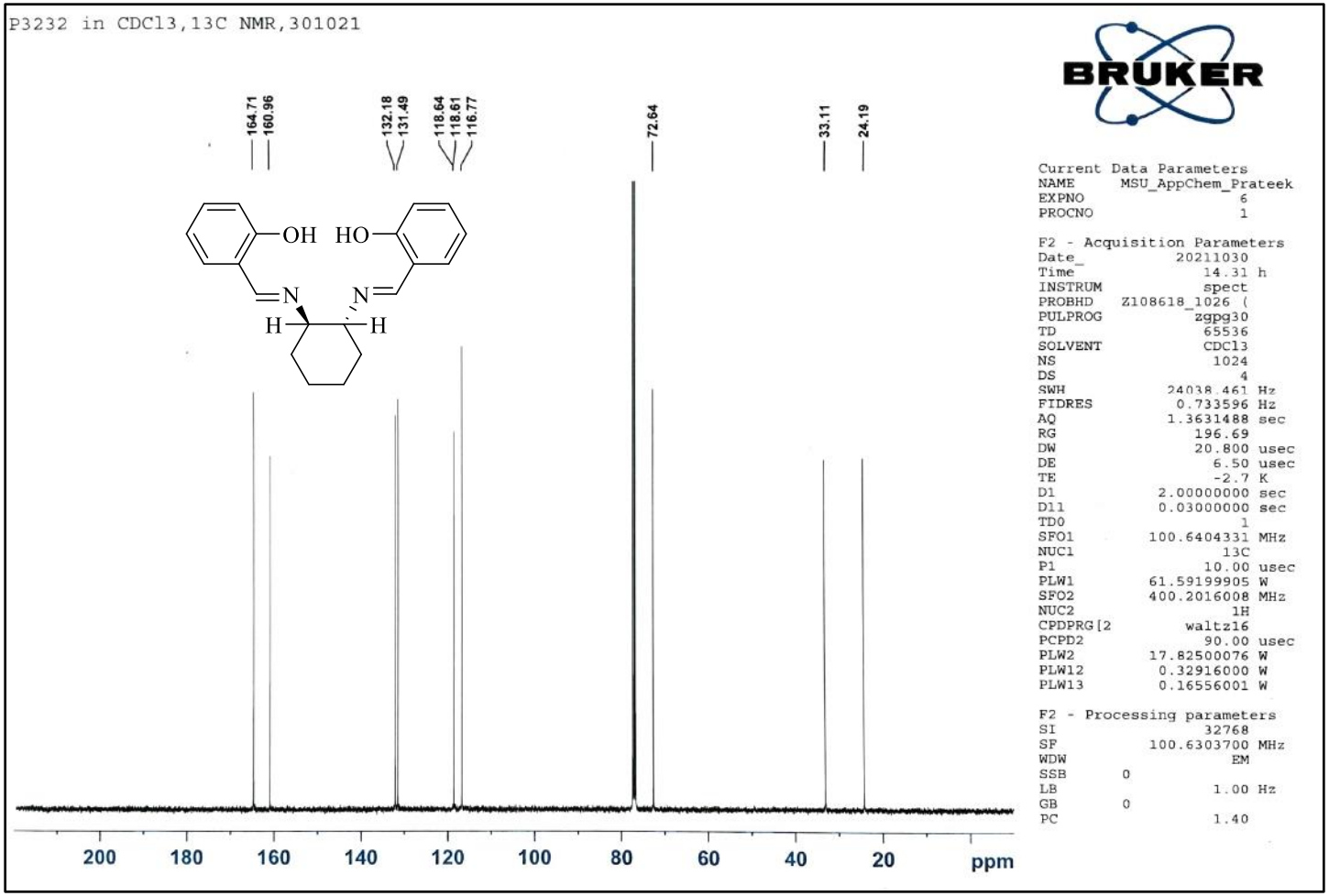

Fig. S2. ^{13}C NMR spectra of the salen ligand.

^{13}C NMR spectra of the salen complex. ^{13}C NMR (100 MHz, $CDCl_3$): δ (ppm) =164.71, 160.96, 132.18, 131.49, 118.64, 118.61, 116.77, 72.64, 33.11, 24.19.

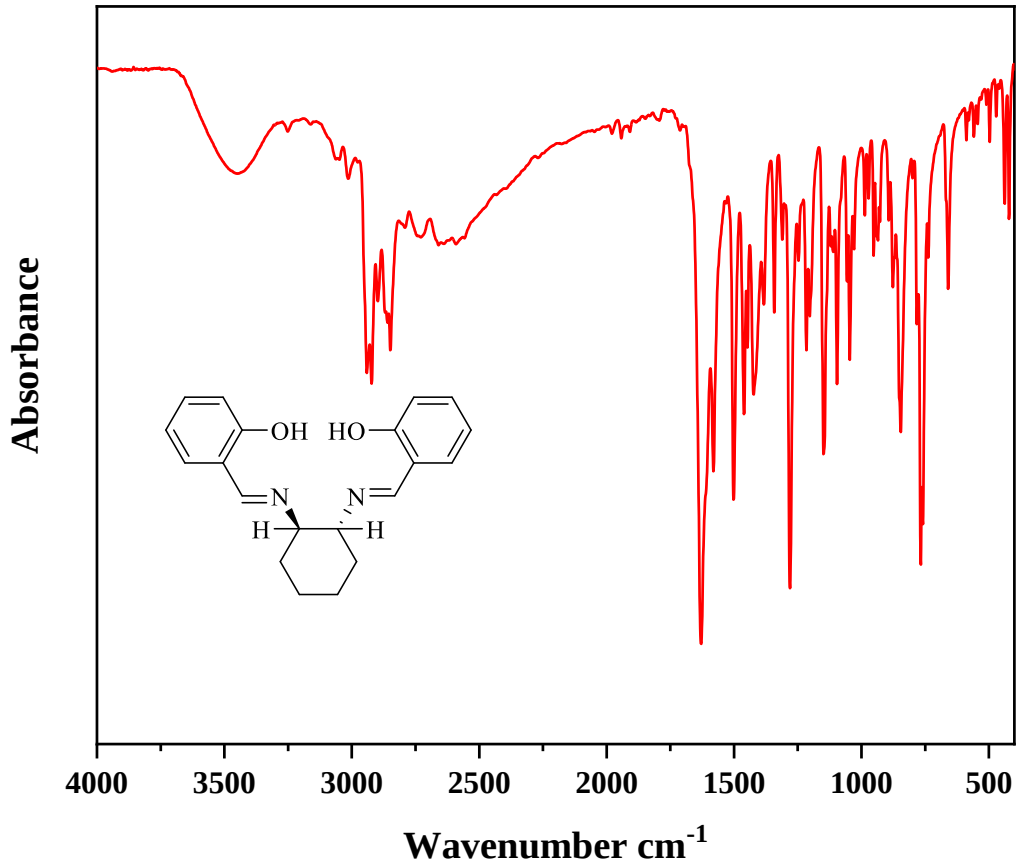

Fig. S3. FTIR spectra of the salen ligand.

4. Characterization Data for Catalyst

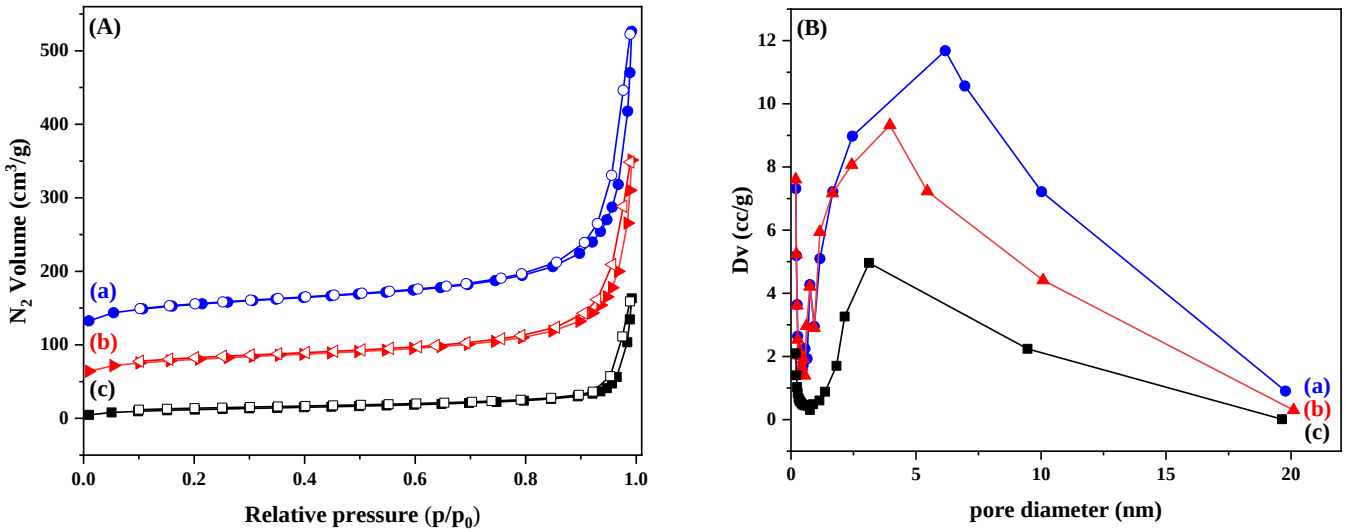

Fig. S4. (A) N_2 adsorption− desorption isotherms of (a) MWW zeolite (b) Cu(II)-MWW zeolite and (c) encapsulated chiral Cu(II) salen catalyst; **(B)** BJH pore size distributions of (a) MWW zeolite (b) Cu(II)-MWW zeolite and (c) encapsulated chiral Cu(II) salen catalyst**.**

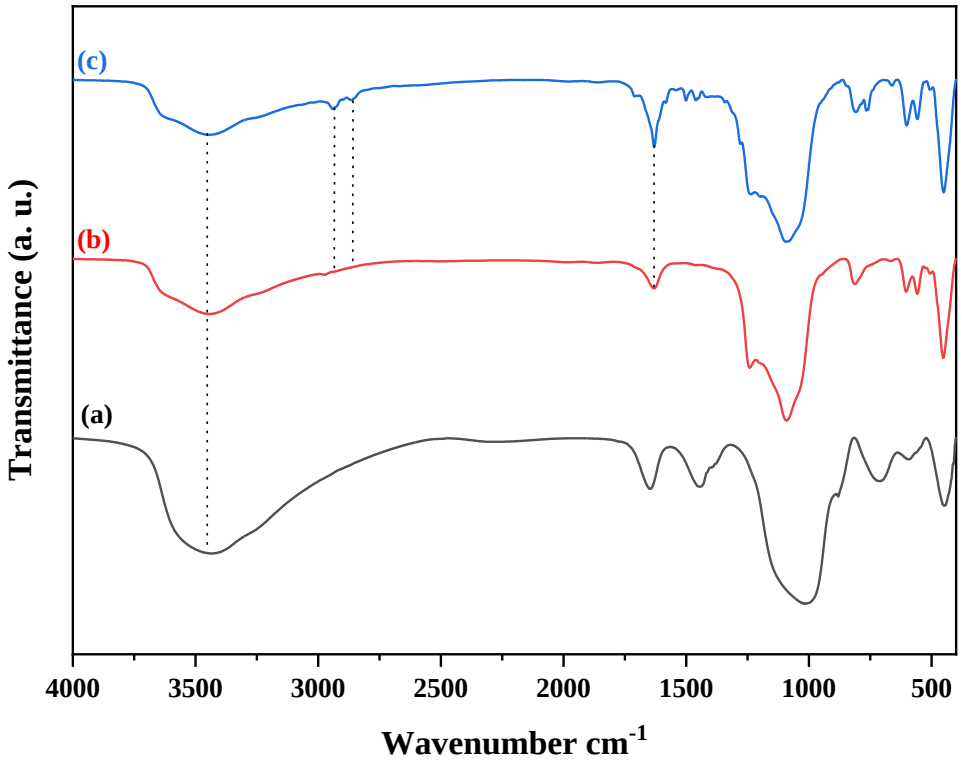

Fig. S5. FTIR spectra of (a) MWW zeolite; (b) Cu(II) MWW zeolite; (c) Encapsulated chiral Cu(II)-salen catalyst.

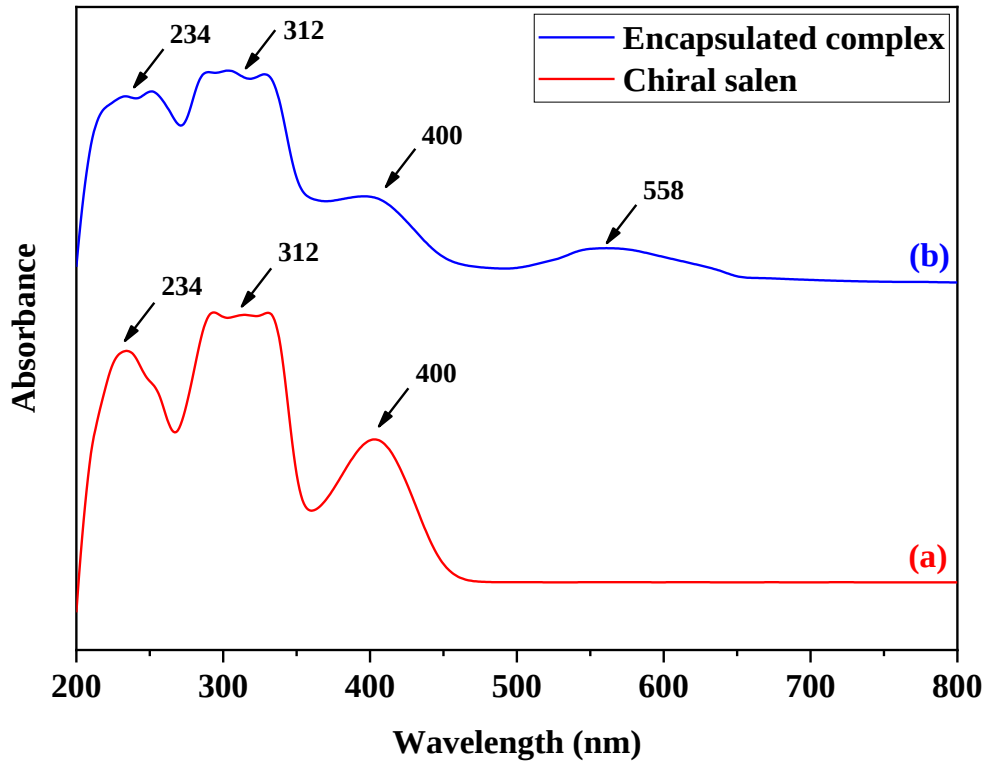

Fig. S6. UV–vis spectra of (a) Chiral salen (b) encapsulated chiral Cu(II) salen

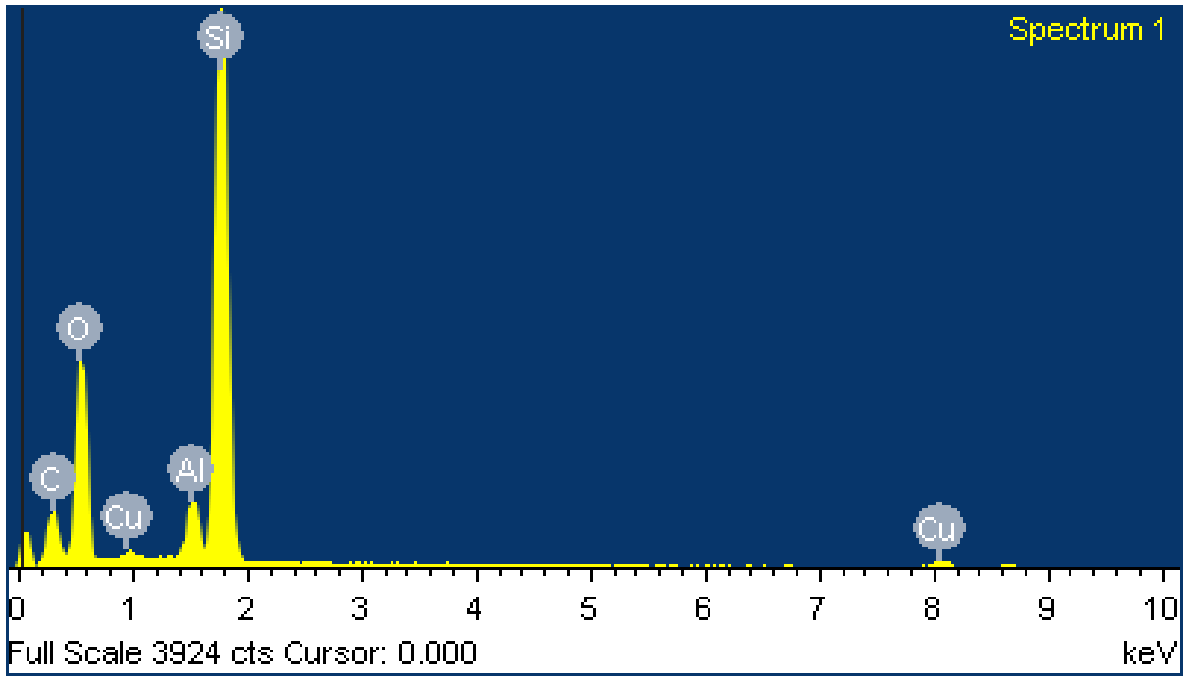

Fig. S7. EDX pattern of encapsulated chiral Cu(II)-salen catalyst

5. Chromatographic data for Products

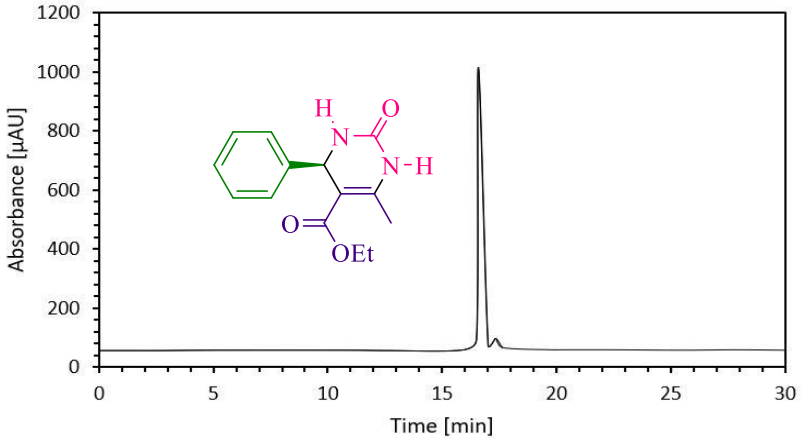

1st cycle of encapsulated chiral Cu(II) salen complex as a catalyst			
Peak	Ret. Time	Area	Area %
1	16.97	10127089	95.96
2	17.25	426289	4.04
Total		10553378	100

Fig. S8. Chiral HPLC spectra of the Benzaldehyde as a reactant.

Column: Chiralpak OJ-H (250 x 4.6) mm, 20µ (make: Diacel), Mobile phase: (n-Hexane and isopropanol (80:20)), Flow rate: 1.0 mL/min, Detection: 280 nm.

Enantiomeric excess (ee%) was calculated from the chromatographic data by the following equation:

$$(ee\%) = \left[\frac{peak\ area\ 1 - peak\ area\ 2}{peak\ area\ 1 + peak\ area\ 2}\right] \times 100$$

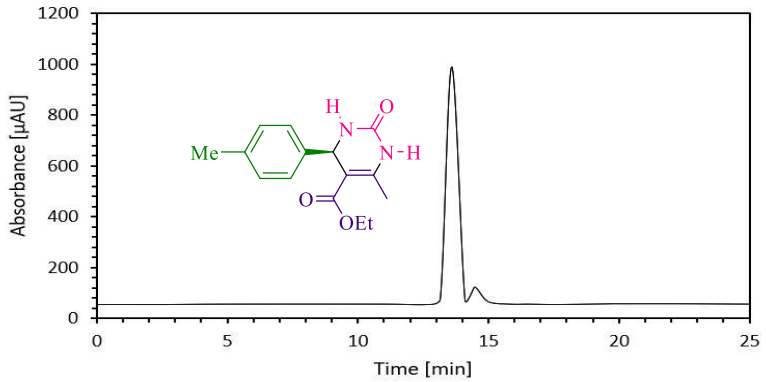

4-Me Benzaldehyde as a reactant			
Peak	Ret. Time	Area	Area %
1	13.59	12015686	93.32
2	14.46	859545	6.68
Total		12875231	100

Fig. S9. Chiral HPLC spectra of the 4-Me Benzaldehyde as a reactant.

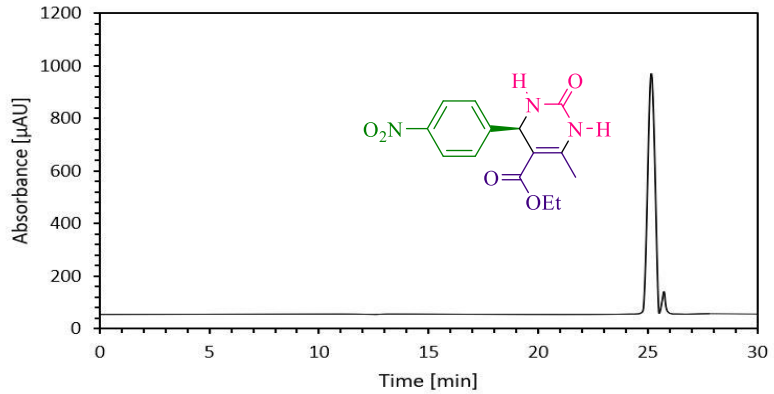

4-NO_2 Benzaldehyde as a reactant			
Peak	Ret. Time	Area	Area %
1	25.36	10256284	91.47
2	25.73	956388	8.53
Total		11212672	100

Fig. S10. Chiral HPLC spectra of the 4-NO_2 Benzaldehyde as a reactant.

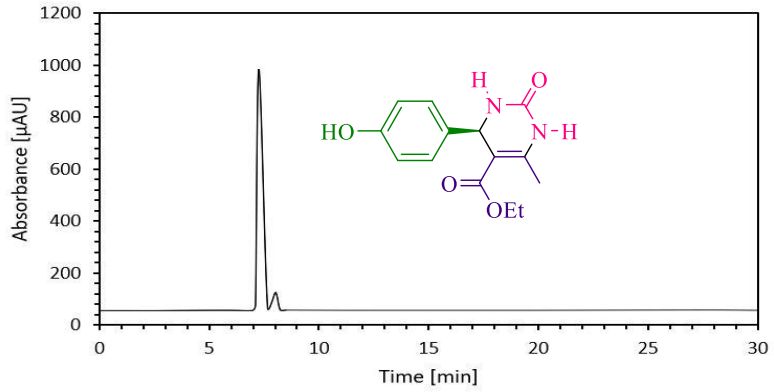

4-OH Benzaldehyde as a reactant			
Peak	Ret. Time	Area	Area %
1	7.35	12016128	92.99
2	8.04	905847	7.01
Total		12921975	100

Fig. S11. Chiral HPLC spectra of the 4-OH Benzaldehyde as a reactant.

6. NMR and FTIR Spectra for Products

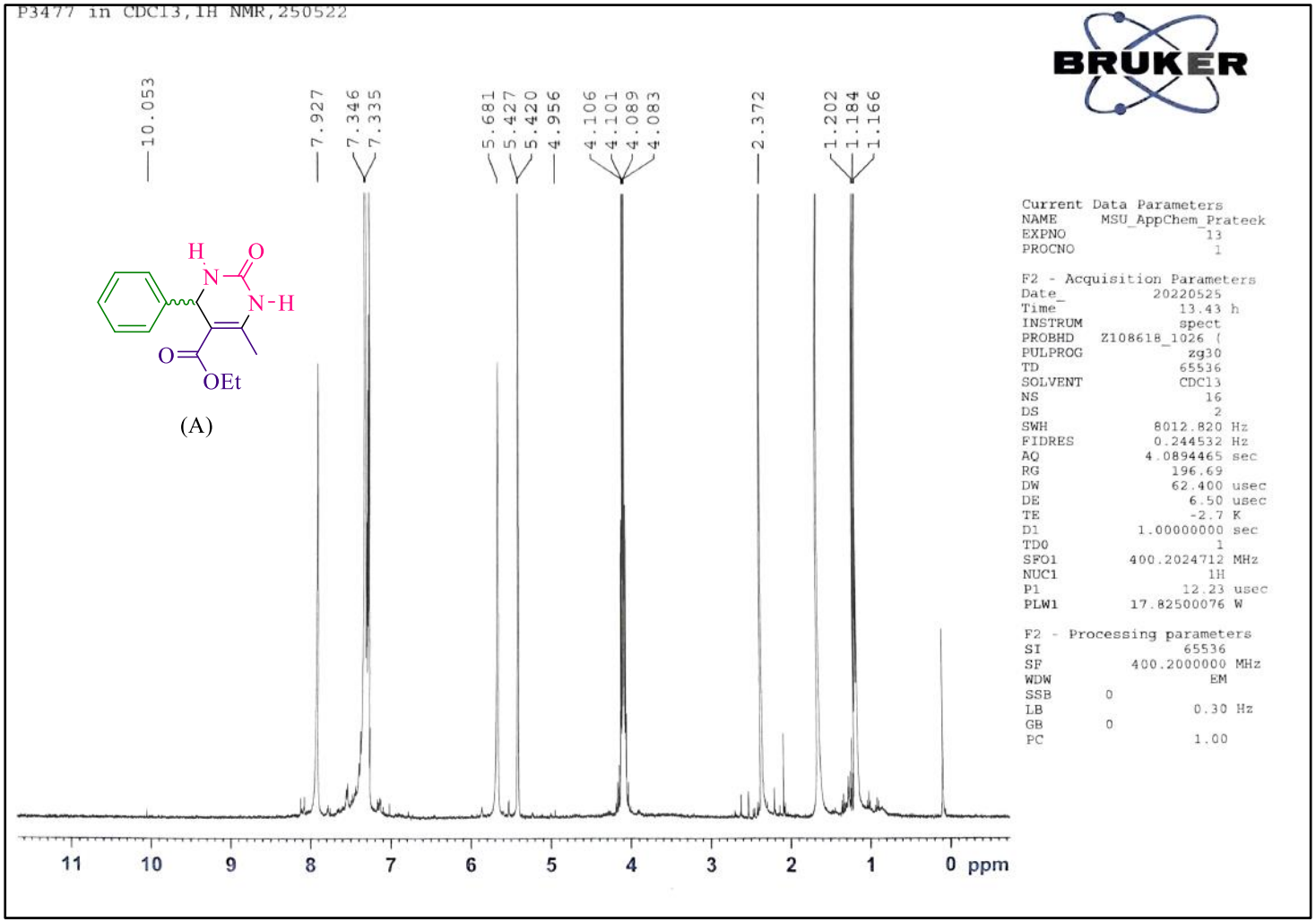

Fig. S12. ^{1}H NMR spectra of the product (A).

^{1}H NMR spectra of the product (A). ^{1}H NMR (400 MHz, $CDCl_3$): δ (ppm) = 7.92−7.33 (m, 5H), 5.68 (s, 1H), 5.42 (s, 1H), 4.10−4.08 (m, 1H), 2.37 (q, 2H), 1.20 (d, 3H), 0.93 (t, 3H).

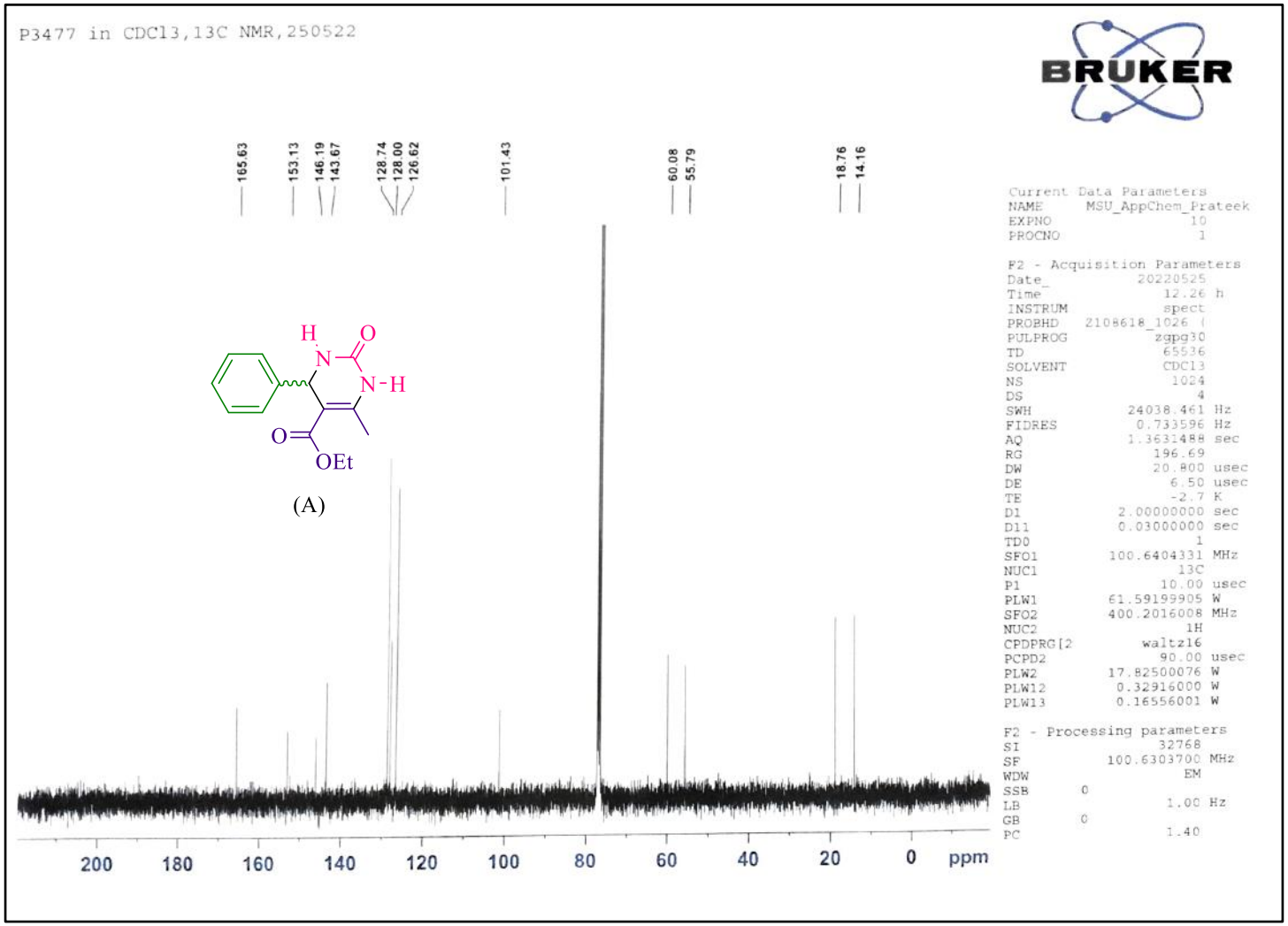

Fig. S13. ^{13}C NMR spectra of the product (A).

^{13}C NMR spectra of the product (A). ^{13}C NMR (100 MHz, $CDCl_3$): δ (ppm) = 165.63, 153.13, 146.19, 143.67, 128.74, 128.00, 126.62, 101.43, 60.08, 55.79, 18.76, 14.16.

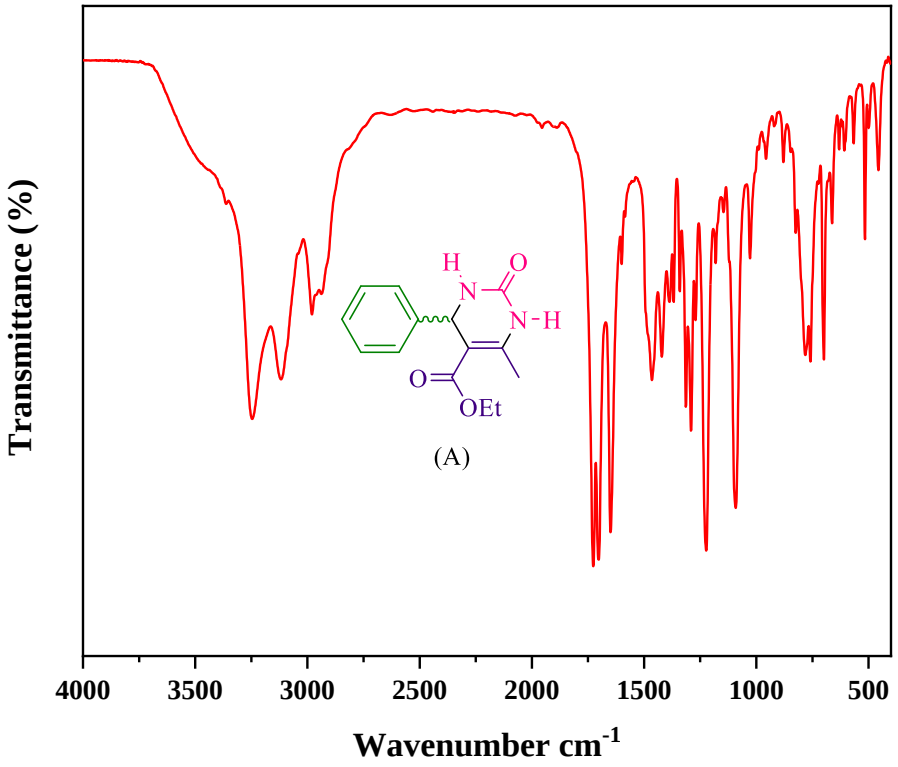

Fig. S14. FTIR spectra of the product (A).

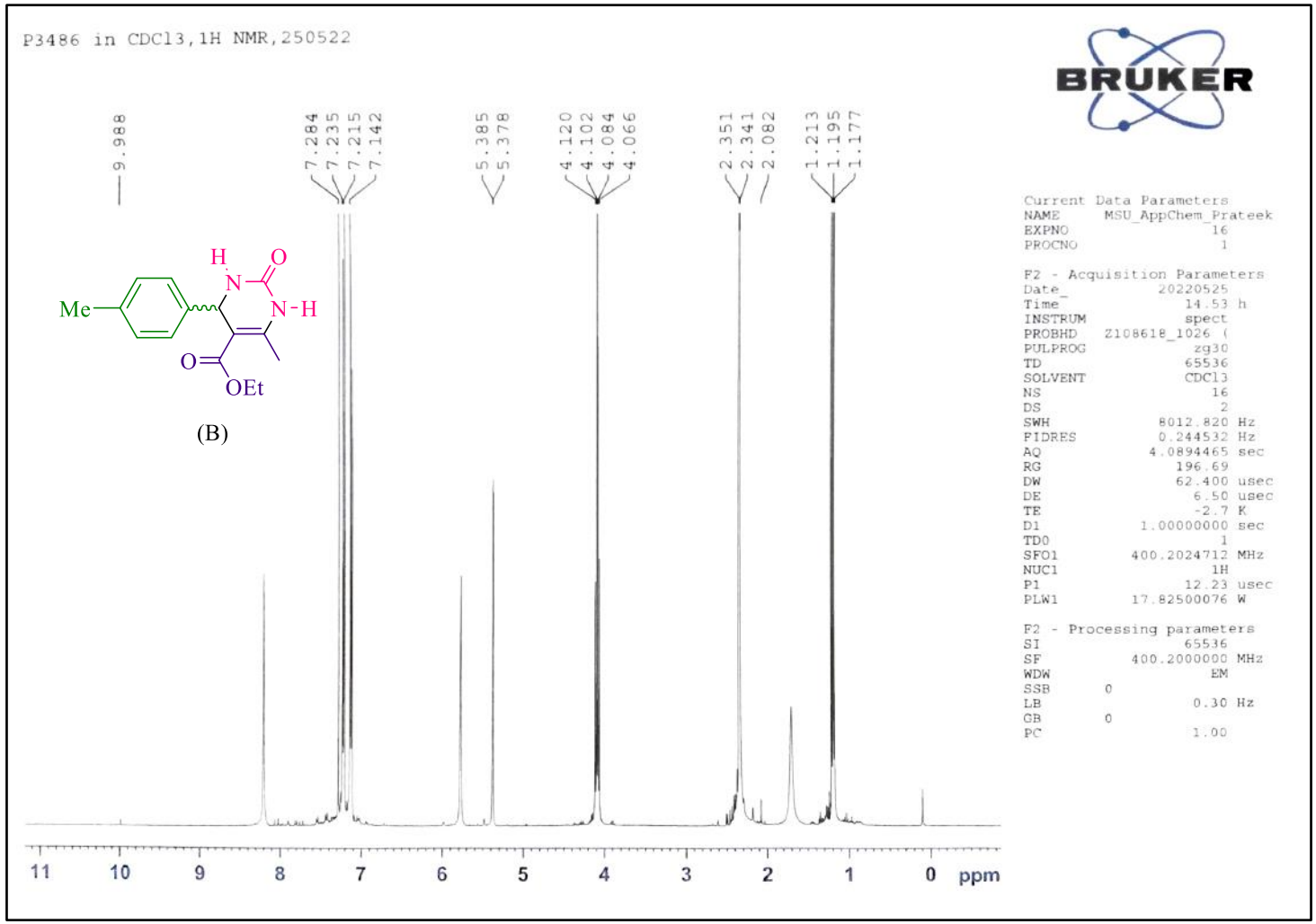

Fig. S15. ^{1}H NMR spectra of the product (B).

^{1}H NMR spectra of the product (B). ^{1}H NMR (400 MHz, $CDCl_3$): δ (ppm) = 9.98 (s, 1H), 7.28 (d, 2H), 7.14 (d, 2H) , 5.38 (s, 1H), 5.37 (d, 1H), 4.10 (q, 2H), 2.35 (s, 3H), 2.08 (s, 3H), 1.19 (t, 3H).

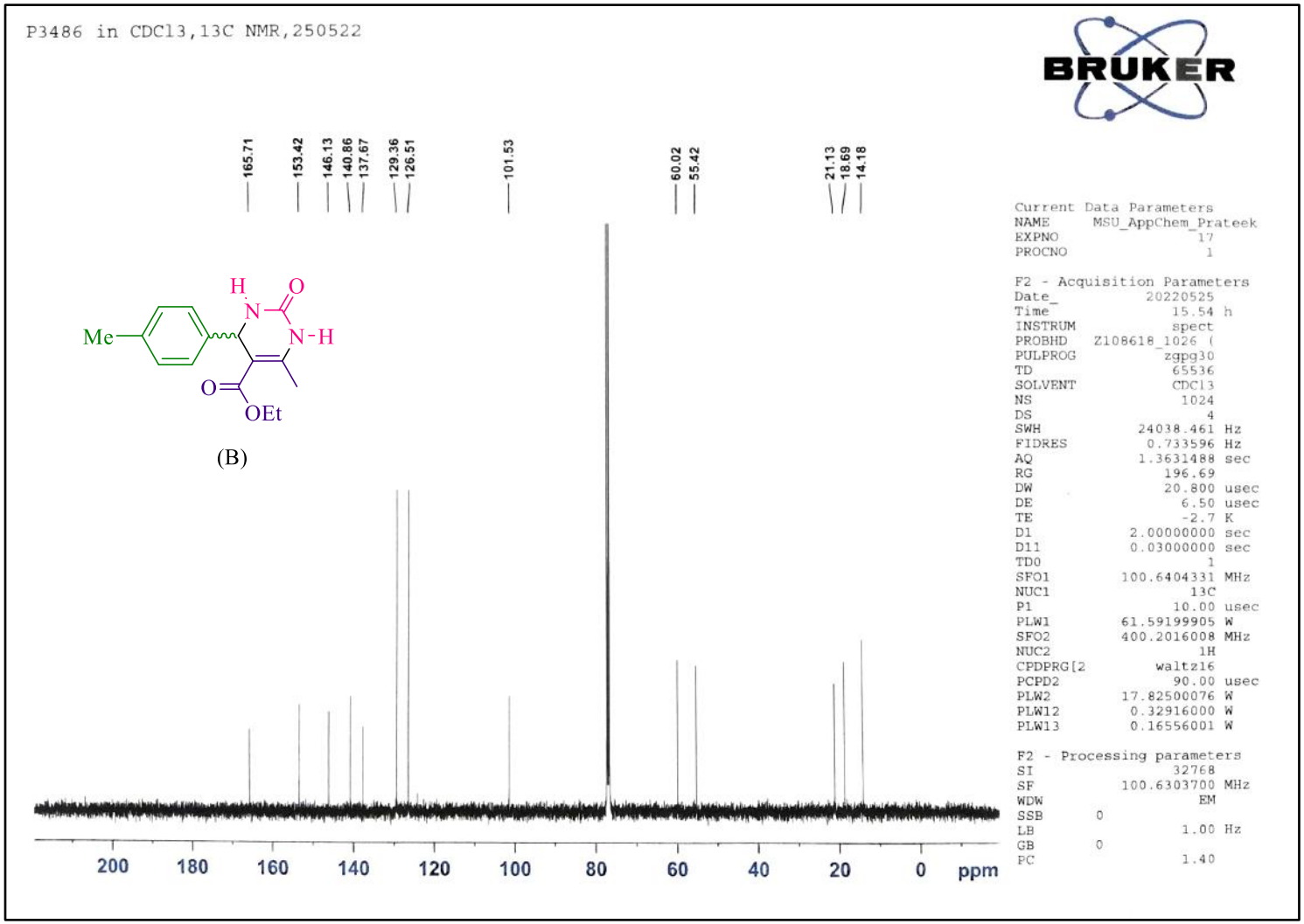

Fig. S16. ^{13}C NMR spectra of the product (B).

^{13}C NMR spectra of the P-Me-Benz product. ^{13}C NMR (100 MHz, $CDCl_3$): δ (ppm) = 165.71, 153.42, 146.13, 140.86, 137.67, 129.36, 129.51, 101.53, 60.02, 55.42, 21.13, 18.69, 14.18.

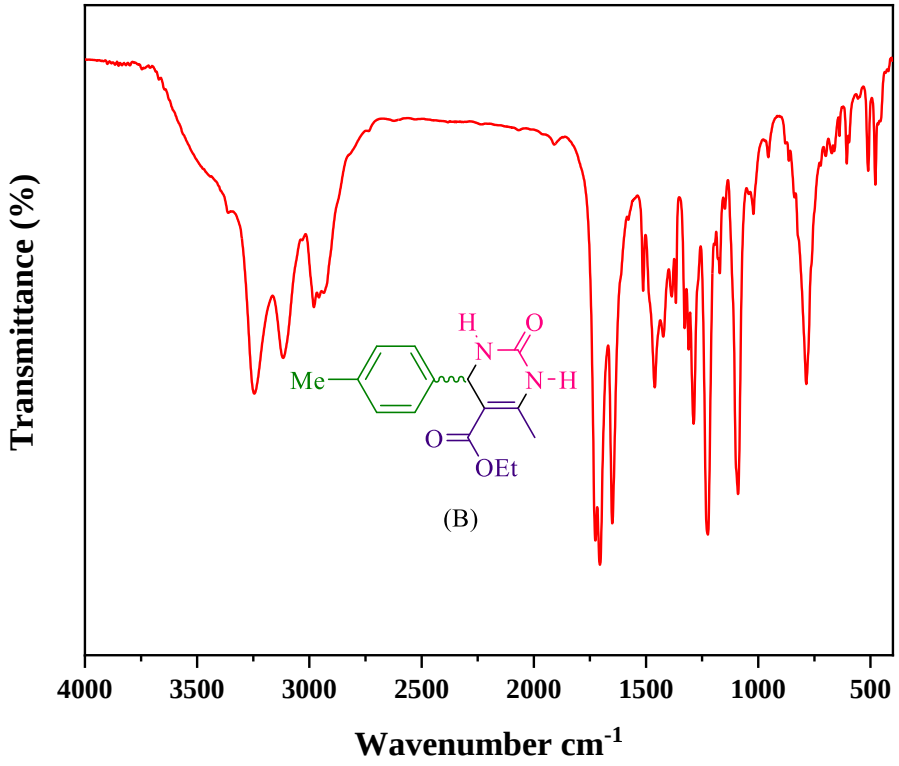

Fig. S17. FTIR spectra of the product (B).

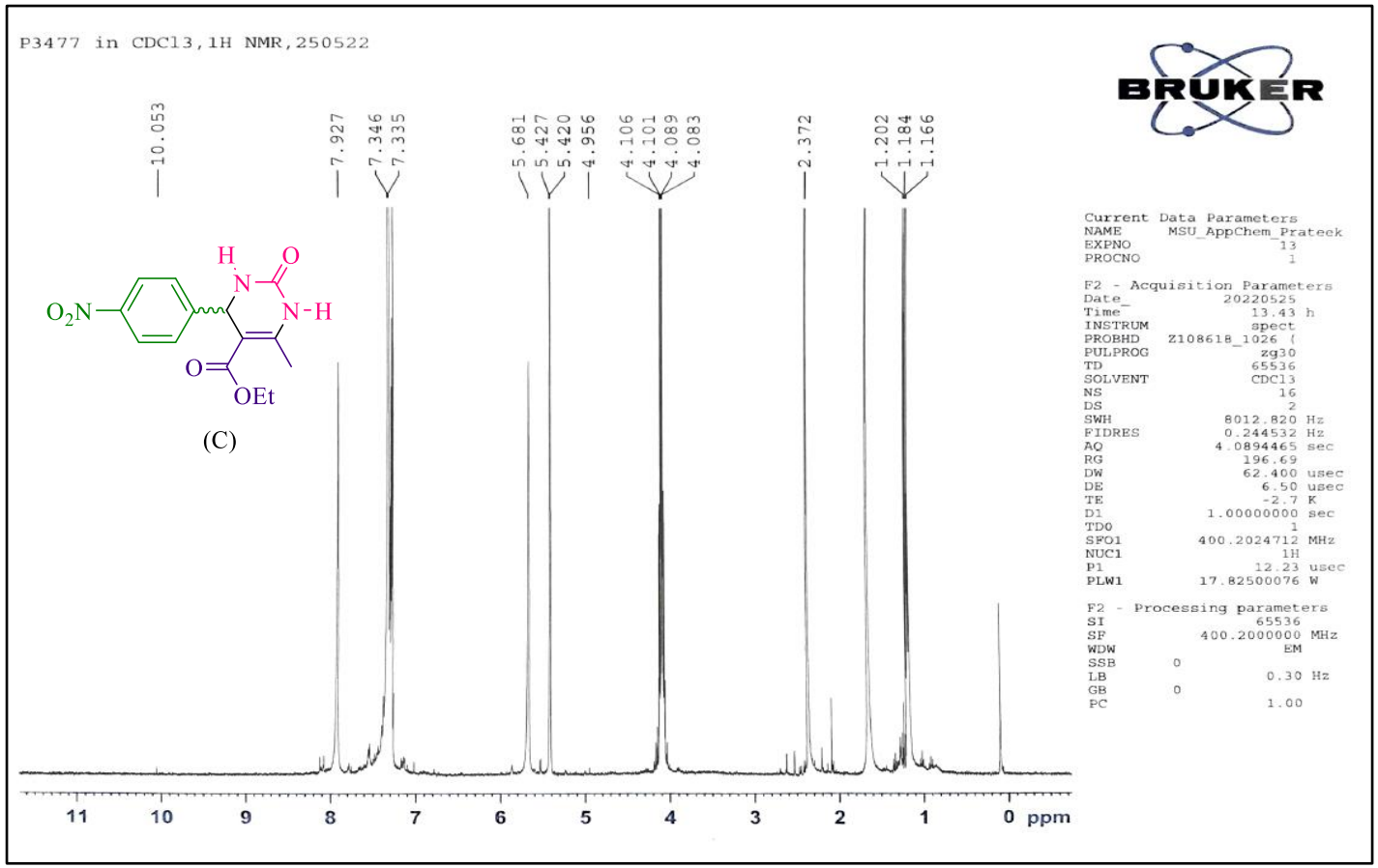

Fig. S18. ^{1}H NMR spectra of the product (C).

^{1}H NMR spectra of the product (C). ^{1}H NMR (400 MHz, $CDCl_3$): δ (ppm) = 10.05 (s, 1H), 8.18-8.20 (m, 2H), 7.92 (s, 1H), 7.33-7.34 (m, 2H), 5.42 (d, 1H), 4.08 (q, 1H), 2.37 (s, 3H), 1.1 (t, 3H).

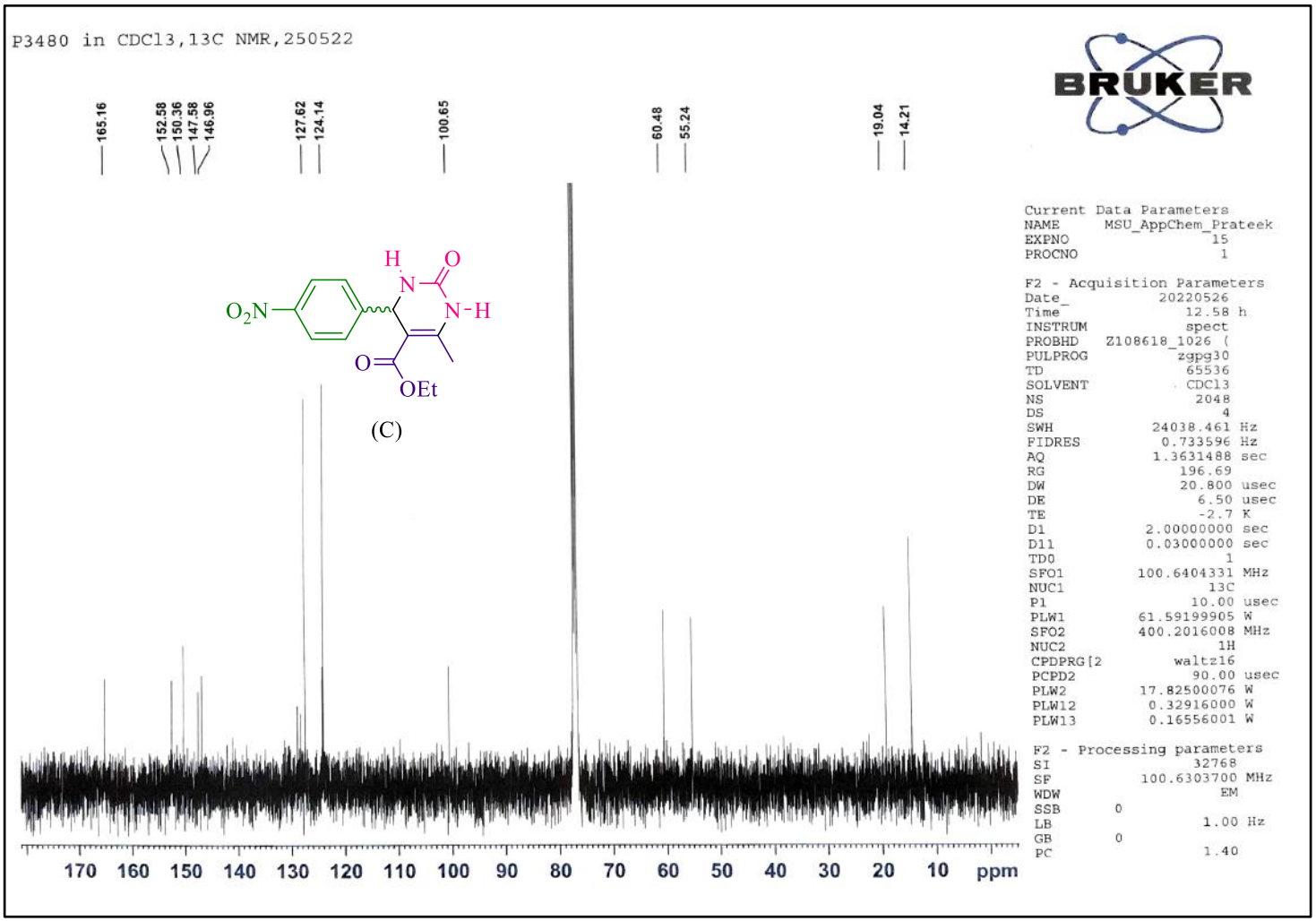

Fig. S19. ^{13}C NMR spectra of the product (C).

^{13}C NMR spectra of the product (C). ^{13}C NMR (100 MHz, $CDCl_3$): δ (ppm) = 165.16, 152.58, 150.36, 147.58, 146.96, 127.62, 124.14, 100.65, 60.48, 55.24, 19.04, 14.21.

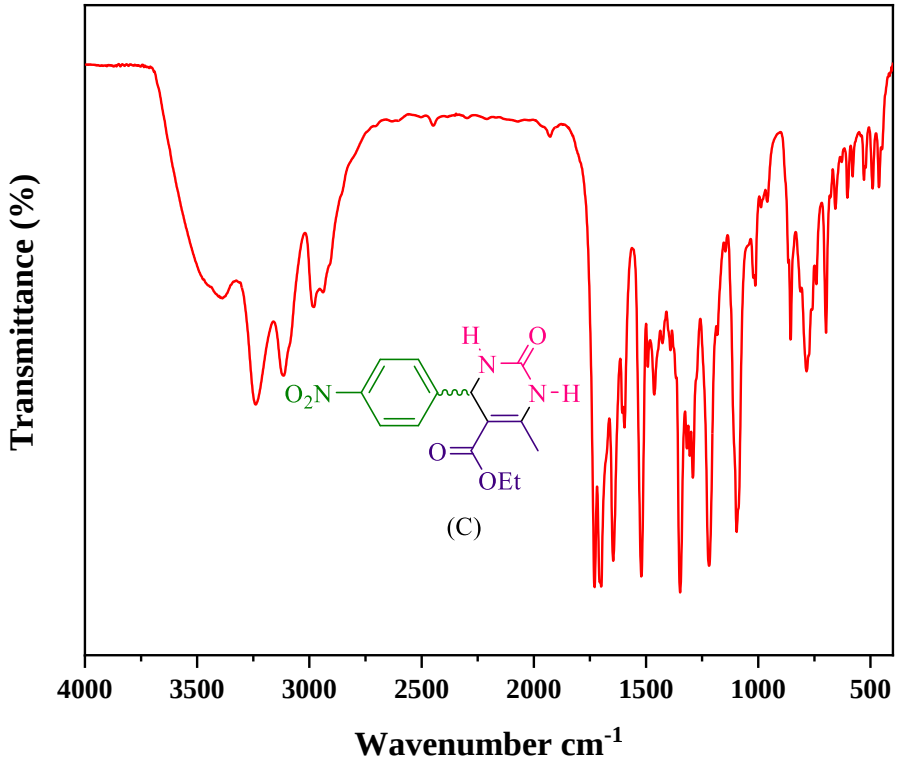

Fig. S20. FTIR spectra of the product (C).

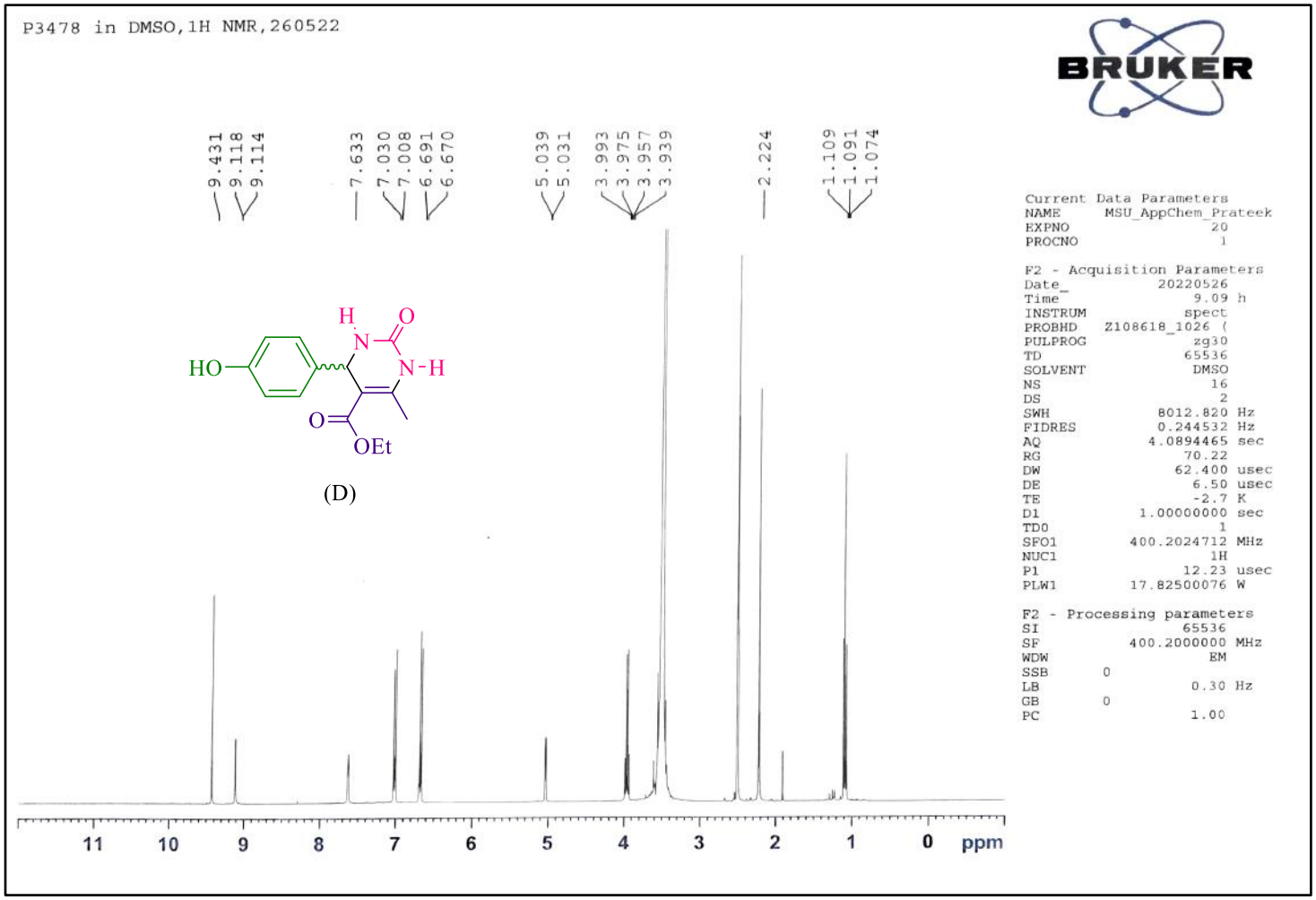

Fig. S21. ^{1}H NMR spectra of the product (D).

^{1}H NMR spectra of the product (D). ^{1}H NMR (400 MHz, $CDCl_3$): δ (ppm) = 9.43(s, 1H), 9.11(s, 1H) 7.63(s, 1H) 7.03-7.00 (d, 1H) 6.69-6.67 (d, 2H), 5.03 (s, 1H), 3.93-3.99 (q, 2H), 2.22 (s, 3H), 1.09 (t, 3H).

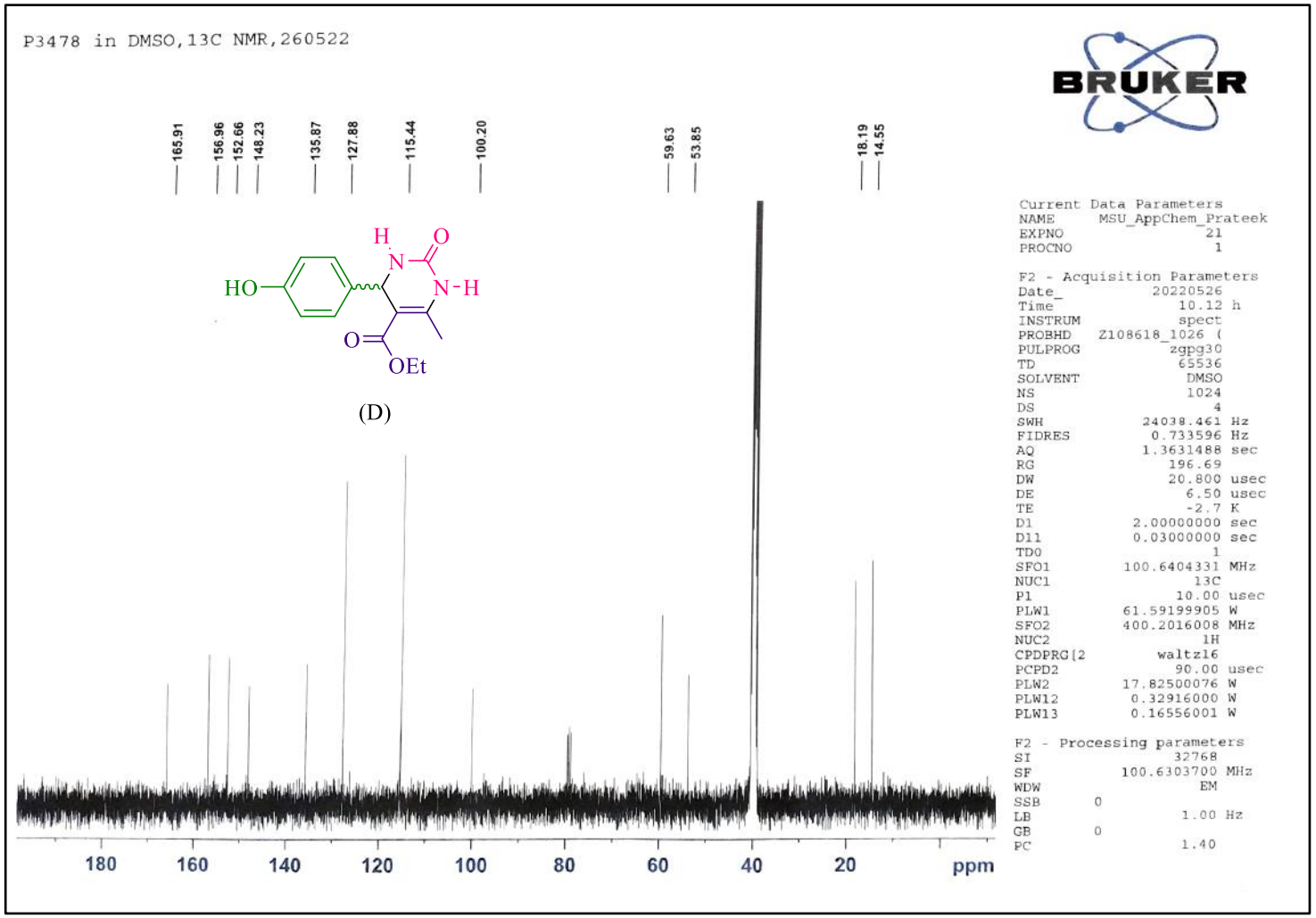

Fig. S22. ^{13}C NMR spectra of the product (D).

^{13}C NMR spectra of the product (D). ^{13}C NMR (100 MHz, $CDCl_3$): δ (ppm) =163.91, 156.96, 152.66, 148.23, 135.87, 127.88, 115.44, 100.20, 59.63, 53.85, 18.19, 14.55.

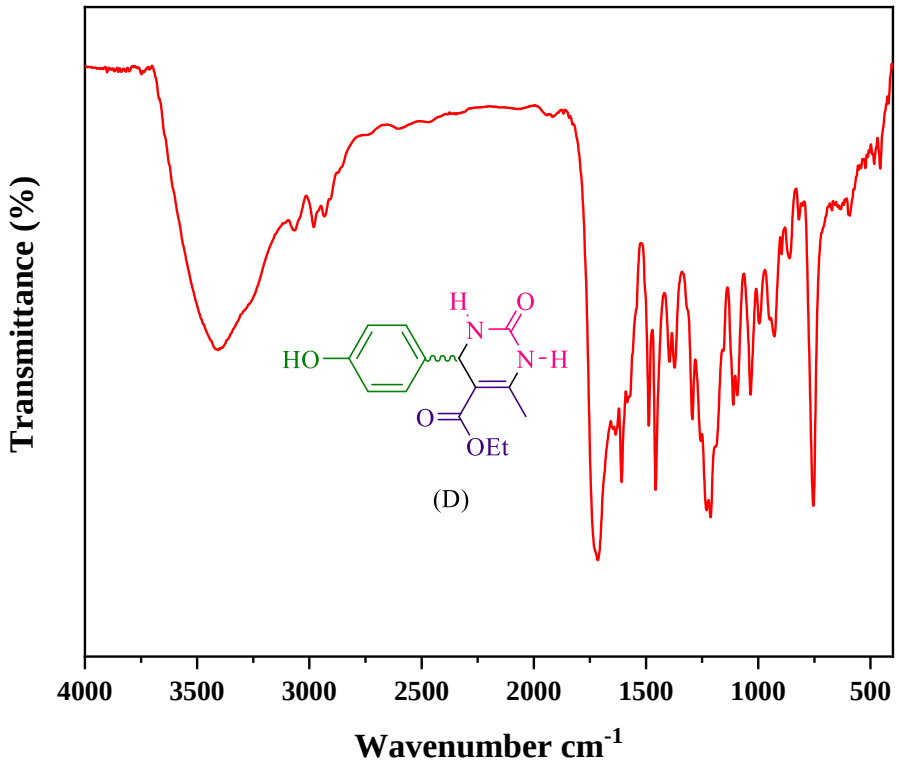

Fig. S23. FTIR spectra of the product (D).

7. Catalyst recyclability bar chart

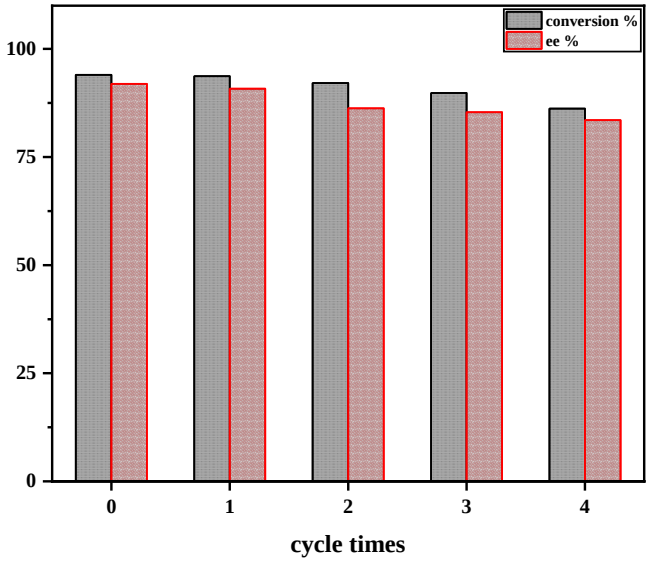

Fig. S24. Recyclability test of encapsulated chiral Cu(II)-salen catalyst over chiral DHPM synthesis.